Dynamical Shock: Cluster results and future studies

KRASNOSELSKIKH Vladimir, ***LPC2E***

LEMBEGE Bertrand, LATMOS;

MAZELLE Christian, CESR

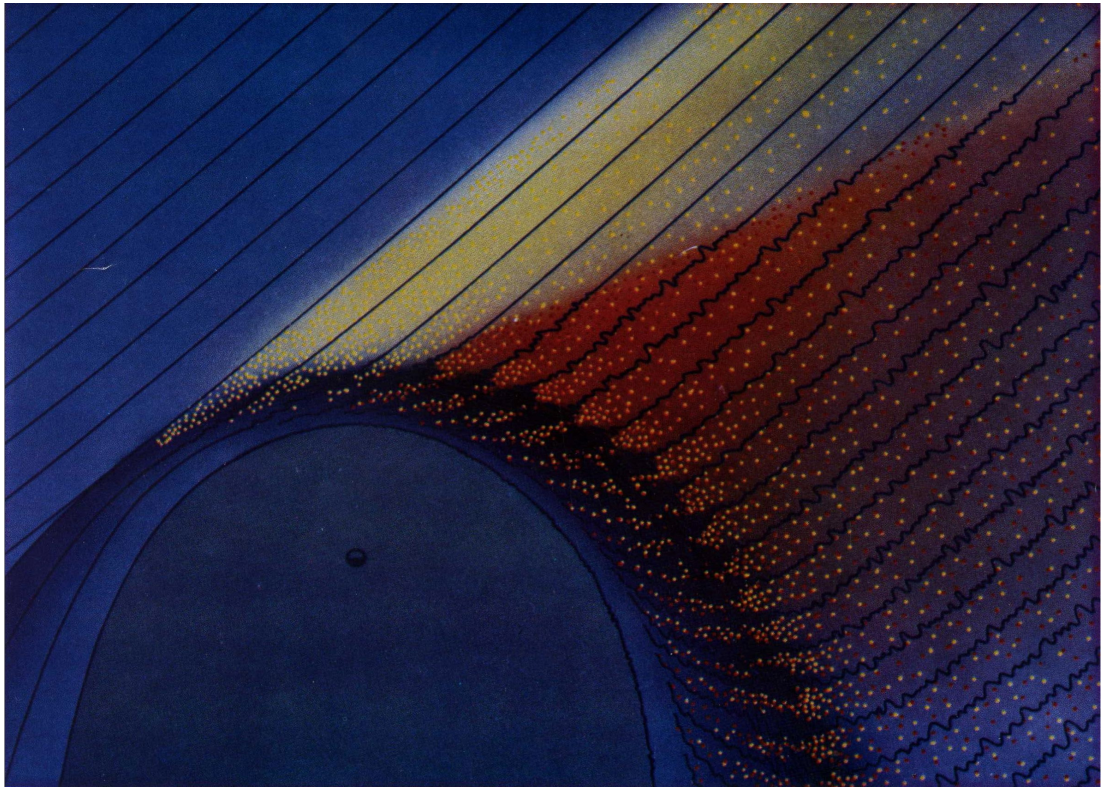

Did Cluster help us in understanding High Mach number shocks?

- ISSI team 2008-2009

- "High-Mach-number collisionless shock dynamics: theory and simulations versus multi-point measurements in space"

- V. Krasnoselskikh
- S. Bale, M. Balikhin, D. Burgess, M. Gedalin, T. Horbury, H. Kucharek, B. Lembege, V. Lobzin, C. Mazelle, S. Schwartz, M. Scholer

- Young scientists:
- J. Soucek, E. Henley, M. Pulupa and A. Tjulin

- H. Comisel

- Three topics:

- Scales
- Sources of upstream wave activity
- Best possible simulation of the 24th January 2001 shock

Structure of the shock front: dispersion versus nonlinearity in the presence of the weak dissipation

Precursors in sub-critical shocks and early models (Sagdeev, 1961, 1964)

The structure is formed as a result of counter-balance between nonlinearity and dispersion, weak dissipation

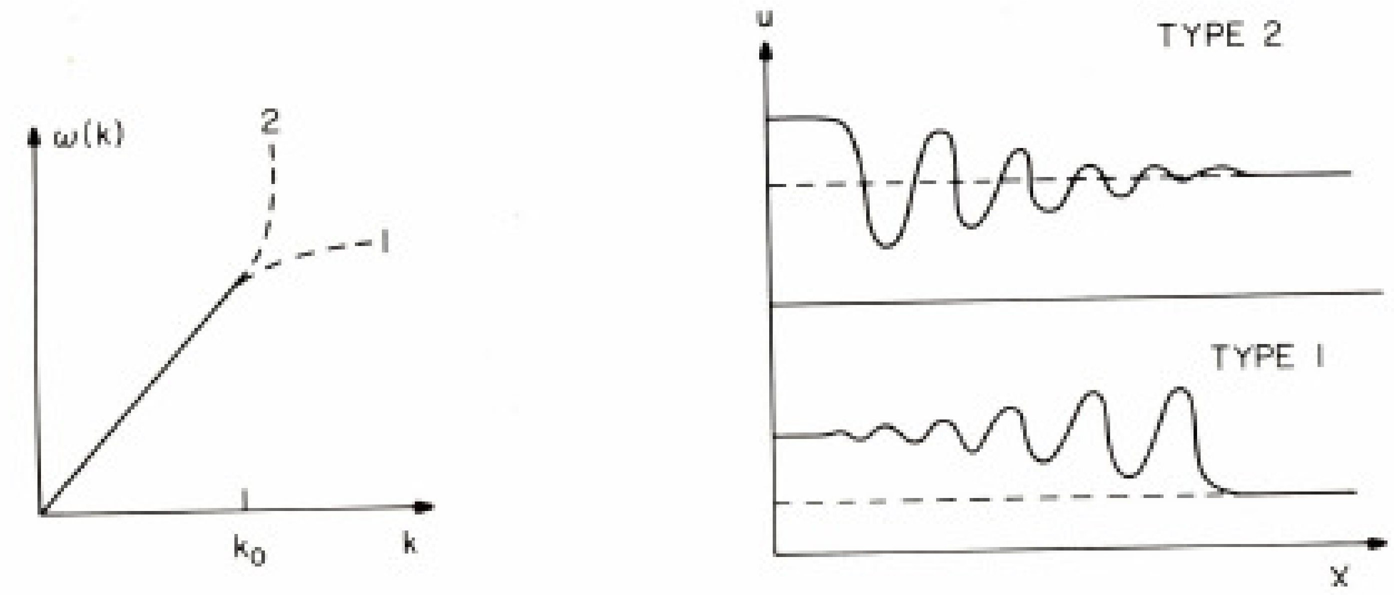

Fig. 3. (Left) Dispersion relation types. (Right) Resulting shock structures. Traces on the right represent the evolution of an unspecified shock parameter from initial upstream conditions (to the far right) to final downstream values ($x = 0$) [after *Biskamp*, 1973].

High Mach number shocks are supposed to become non-stationary
What are possible reasons for nonstationarity and reformation?

- *Three possibilities*

- *I. Domination of the nonlinearity over dissipation when the dispersion is negligible, in other words, the dissipation mechanism is not capable to ensure necessary energy transformation*

- *II. Due to the dynamics of instabilities in the foot region (simulations)*

- *III. Instability of the shock front ramp due to the domination of the nonlinearity over dispersion, when the shock front (ramp region) is formed as nonlinear dispersive structure*

Standing whistler ?

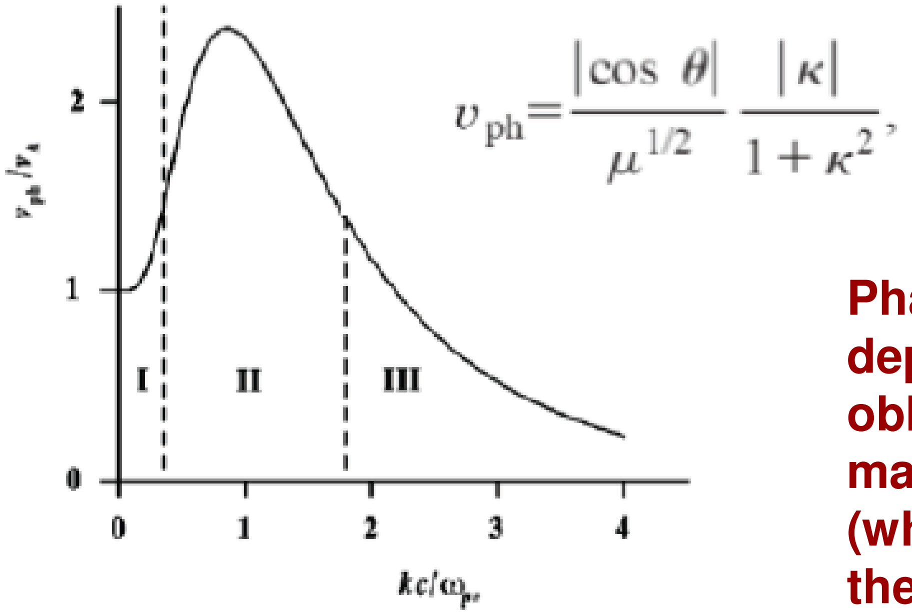

Phase velocity dependence of oblique fast magnetosonic (whistler) waves upon the wavenumber

- There is a maximum v_{ph}/V_A for whistlers
- There is a maximum M for which whistler can stand
- High-Mach numbers: non-stationarity inevitable

From Krasnoselskikh et al. (2002)

Galeev et al., 1988 a,b,c; Krasnoselskikh et al. 2002

Gradient catastrophe of nonlinear upstream whistler

Above whistler critical Mach number whistler precursor becomes nonlinear

Nonlinear whistler critical Mach number

$$M_{nw} = \frac{|\cos\Theta_{Bn}|}{(2m_e/m_i)^{1/2}}$$

Above M_{nw} shock nonlinear steepening of waves can not be stopped anymore by dispersion and/or dissipation and becomes non-stationary

Reformation process

Laboratoire de Physique et Chimie de l'Environnement

- Steepening in time that means the appearance of small scales (several (c/ω_{pe}))
- Overturning, also called « gradient catastrophe » of the « old » front, and, as a consequence, « bursty » ion reflection
- Formation of the « new » front and return to the beginning
- Many factors that are not taken into consideration

Appeal to experimental data of multi-point measurements: Cluster

What are the right questions to answer making use of the data?

- Does the front steepen with the growth of the Mach number till the scales comparable with electron inertial length?
- What are the characteristic scales of fine structure of the shock front?
- What are the sources of waves observed upstream of the ramp?
- Can we observe direct manifestations of the overturning and reformation?

Cluster: small scale electric field

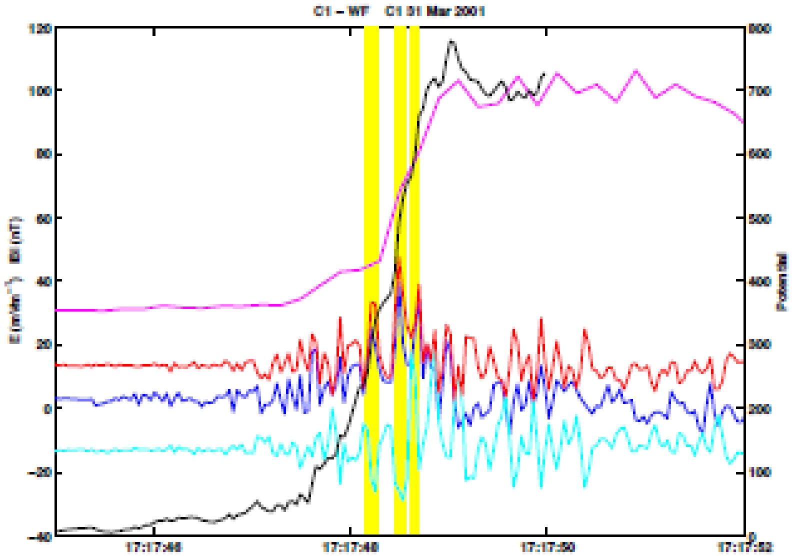

Magnetic and electric field profiles.

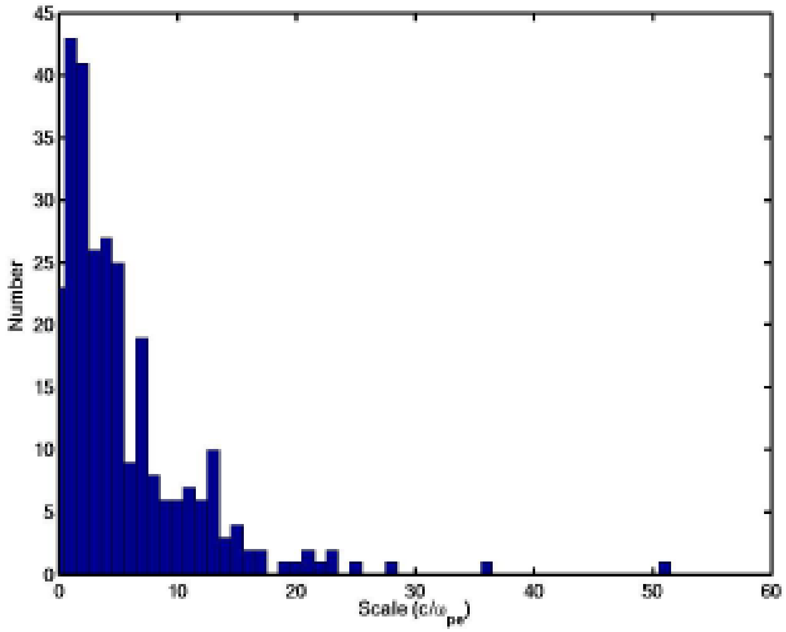

Statistics of the electric spike sizes.

From Walker et al. (2004)

Magnetic field ramp thickness (Hobara et al, 2010)

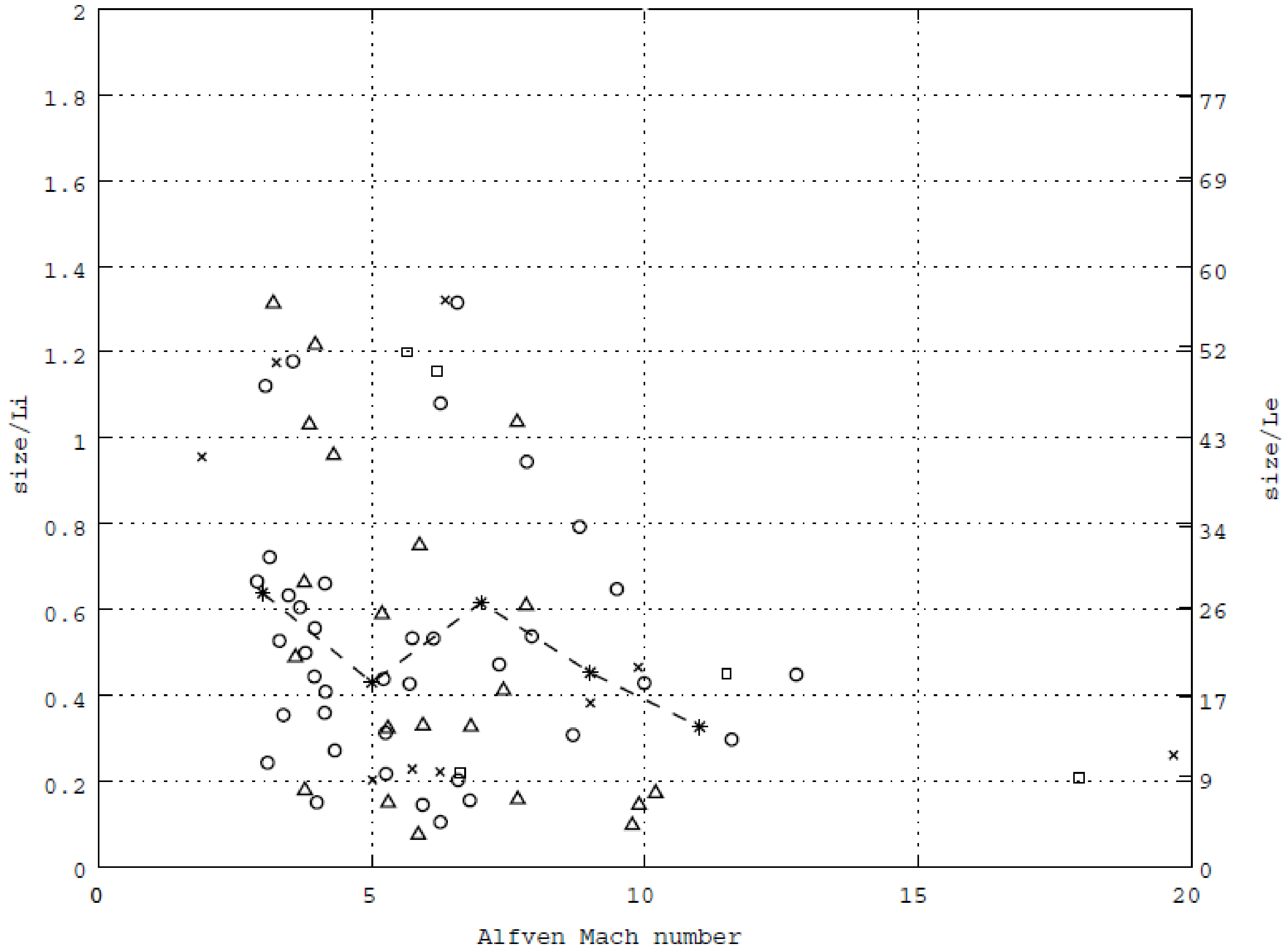

Magnetic ramp thickness statistics (Mazelle et al., 2009)

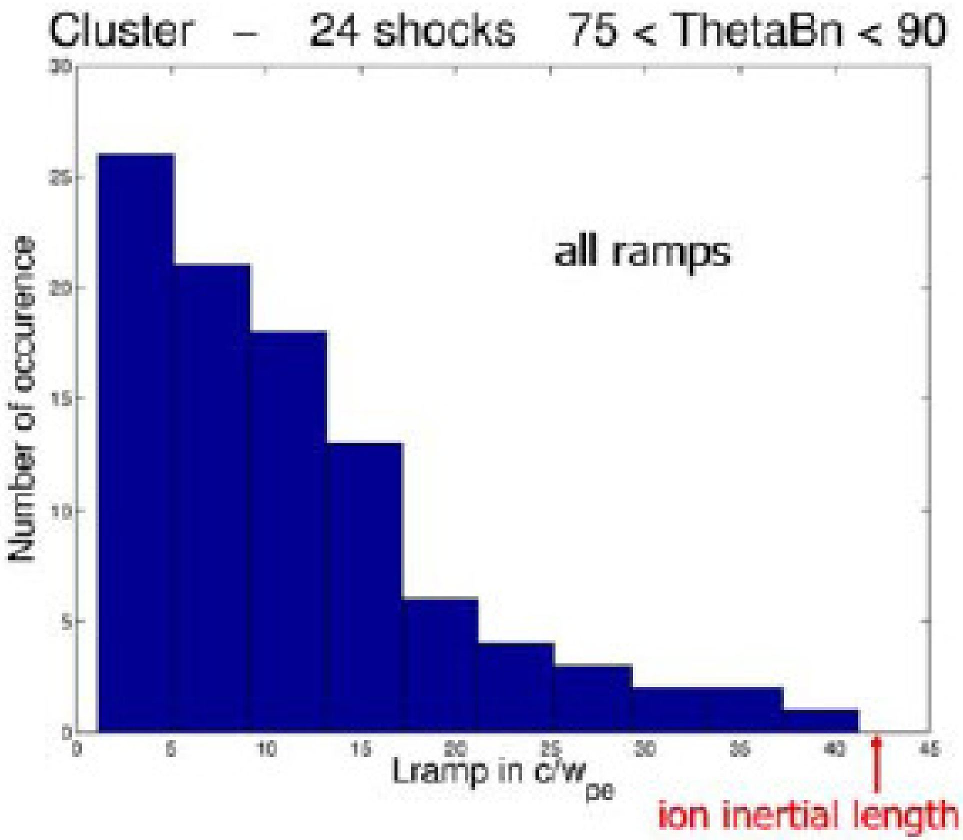

FIGURE 6. Histogram of the 96 shock ramp thicknesses.

Whistler: energy flux

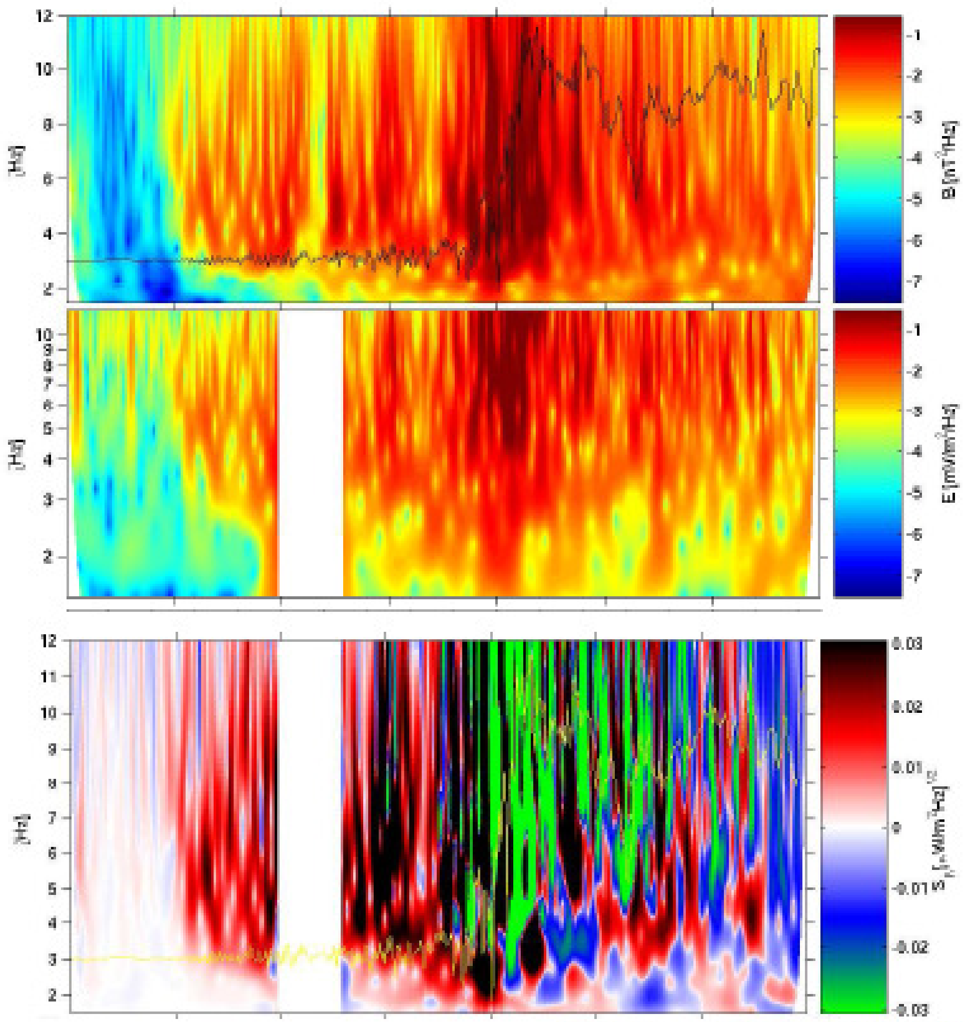

Energy flux by upstream waves in a high-Mach $M \sim 4$ nearly-perpendicular $\theta_{Bn} \sim 85^\circ$ shock:
(top) Power spectra of the magnetic field
(middle) Power spectra of the electric field
(bottom) Projection of the Poynting vector, red - toward upstream

From Sundkvist et al. (2010)

Where the waves are generated? Normal Incidence Frame 20/01/2003, M_A=5.5, θ_{Bn} =75.6°, β_i = 0.7 (Sundkvist et al., 2010)

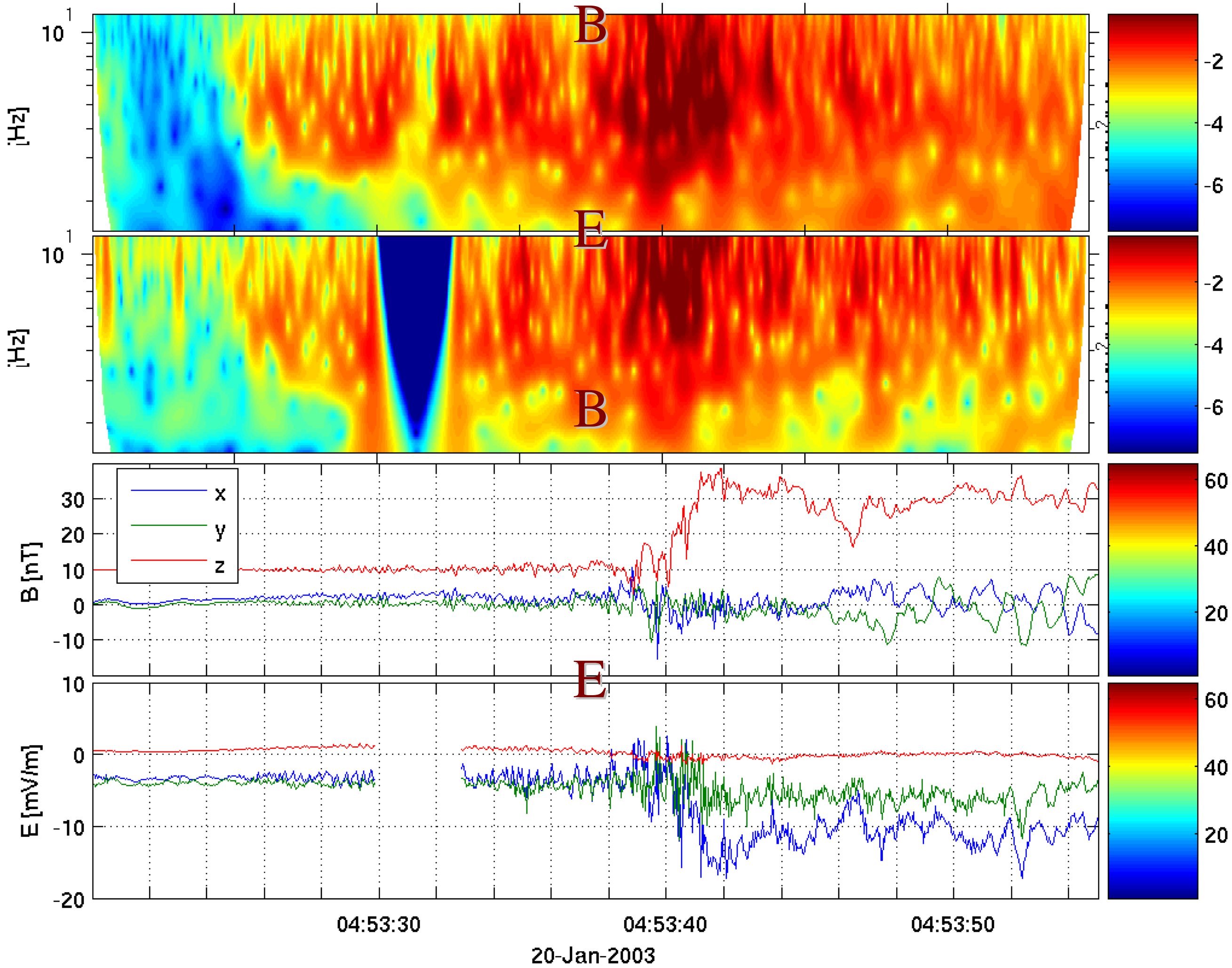

Direct observation of reformation: shock crossing 24 January 2001

Laboratoire de Physique et Chimie de l'Environnement

- *Lobzin,V. V., V. Krasnoselskikh, J.-M. Bosqued, S. J. Schwartz, and M. Dunlop*
- **Nonstationarity and Reformation of High-Mach Number Shocks: Cluster Observations, *Geophys. Res. Lett.*, v. 34, L05107, doi:10.1029/2006GL029095, 2007**

Parameters of the Shock Wave

Laboratoire de Physique et Chimie de l'Environnement

Upstream magnetic intensity	4.21 ± 0.09 nT	**Main Dimensionless Parameters**	
Upstream electron density	9.0 ± 0.2 cm^{-3}	Upstream θ_B	81° ± 4°
Upstream electron temperature	8.2 ± 0.3 eV	Upstream β_e	1.7
Frequencies, Periods and Characteristic Lengths		Upstream β_i	2.0
Upstream electron plasma frequency f_{pe}	27.0 ± 0.3 kHz	Alfvén Mach number M_A	10
Upstream electron Debye length λ_{De}	5 m	Fast Mach number M_f	5
Upstream proton gyroperiod T_{Bi}	15.5 s		

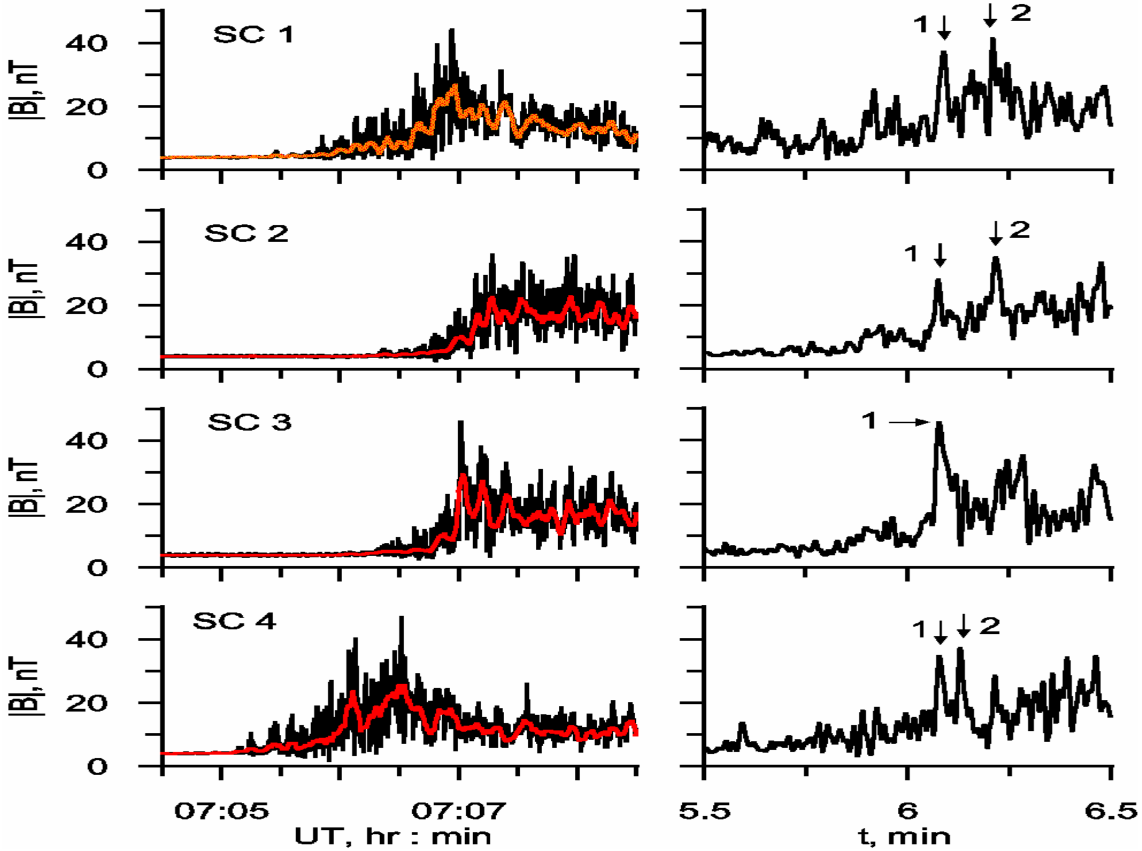

The magnetic field profiles obtained by FGM experiments aboard Cluster spacecraft during the Earth's bow shock crossing on January 24, 2001 (Lobzin et al. 2007).

Hodograms for magnetic field peaks

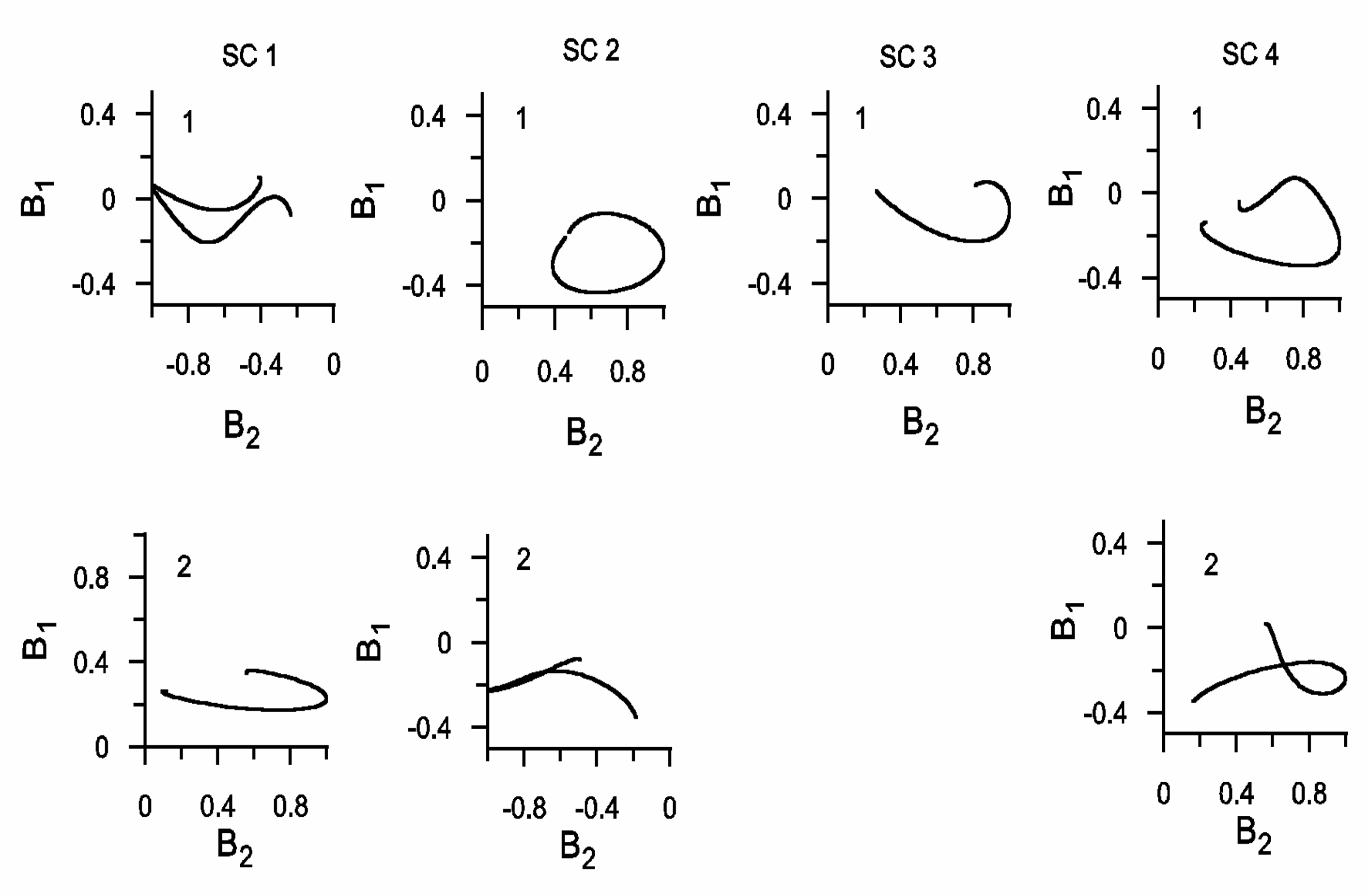

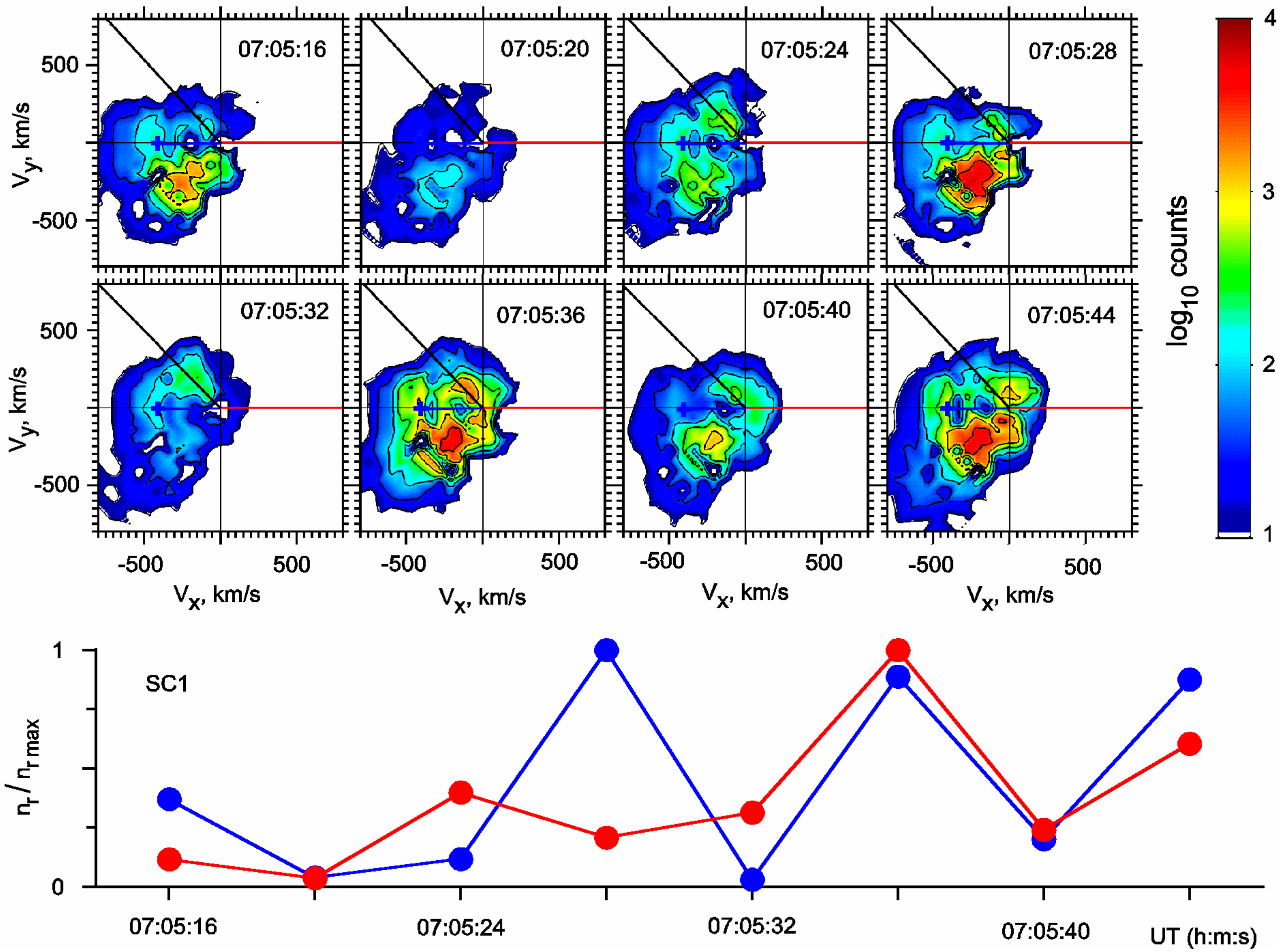

The ion velocity distributions in the forward part of the foot for the bow shock crossing on 24 January 2001 and temporal variations for relative number of counts corresponding to reflected ions (*Lobzin et al.* 2006).

Conclusions

- The magnetic profile of high-Mach number shocks steepens down to the scales much smaller than the ion inertial length and may approach the electron inertial length
- Electric field scales within the ramp are typically smaller than the magnetic scales, related to electron processes (yet to be fully understood)
- Magnetic steepening is nonlinear and is stopped by dispersion (in stationary regime) when (nonlinear) whistler is formed.
- Steepening cascades energy to small scales, the energy is taken away from the shock by the whistler
- Above some critical Mach number the whistler is unable to take away the energy and the shock becomes reforming

Conclusions II

The most probable reason for reformation is related to weakness of the dispersion that can not stop nonlinear steepening

In the case of oblique quasiperpendicular shocks the critical Mach number for the transition from stationary to nonstationary dynamics can be evaluated using the condition that the whistler precursor wave train can not be anymore established upstream of the shock ramp

- Computer simulations by means of the PIC codes can not properly model physical processes of the particle interaction with fields because they artificially overestimate electric to magnetic fields ratio

Shocking astrophysics

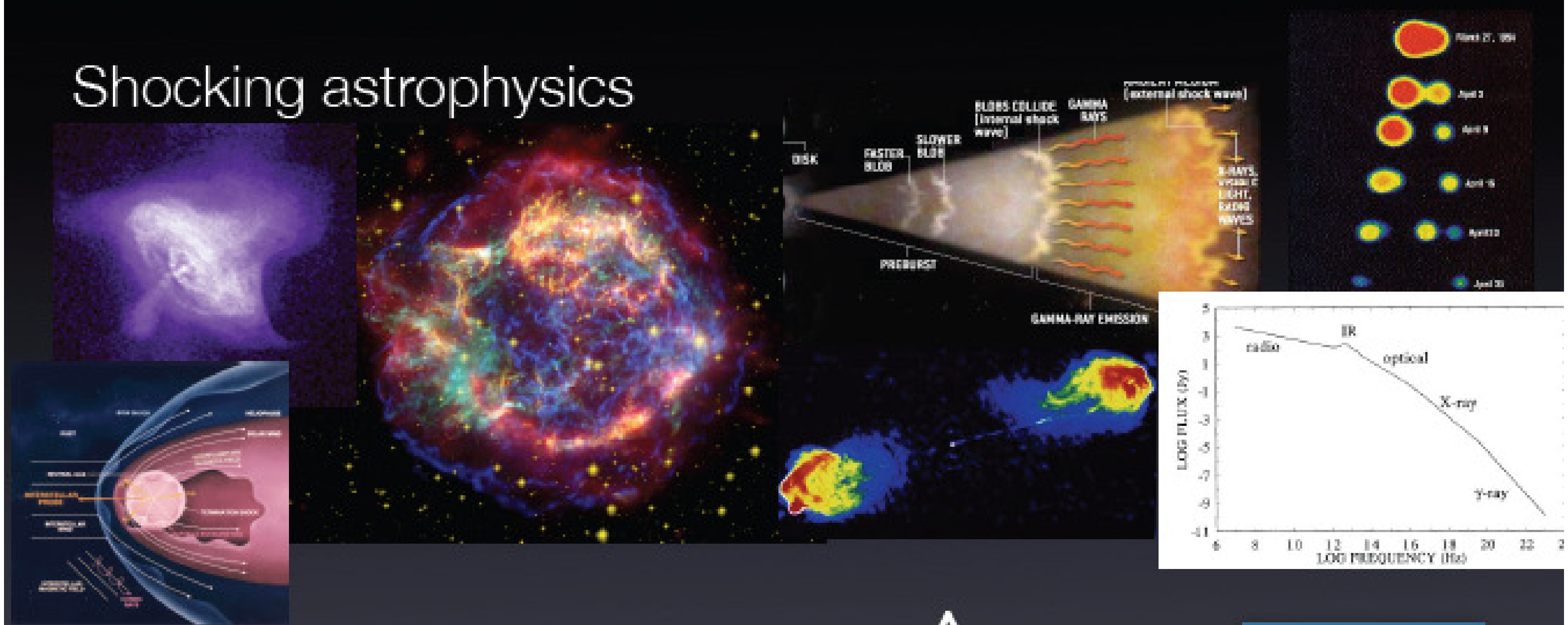

Shocks span a range of parameters:
nonrelativistic to relativistic flows

magnetization (magnetic/kinetic energy ratio)

composition (pairs/e-ions/pairs + ions)

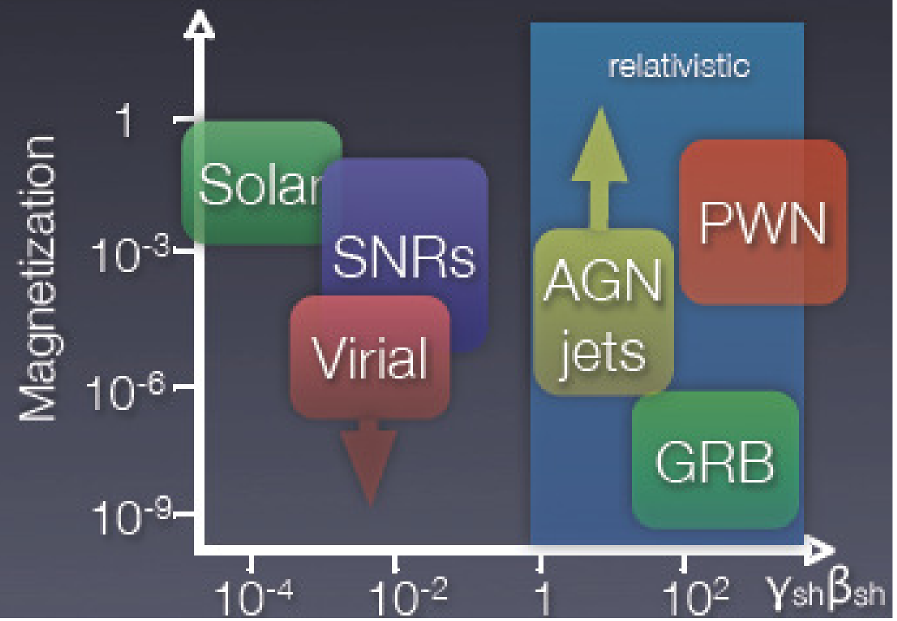

Major differences

Parameter space of collisionless shocks

Properties of shocks can be grossly characterized by several dimensionless parameters:

Alfven Mach number $M_A = \frac{v}{v_A}$

Composition $r = \frac{m_i}{m_e}$

Sonic Mach number $M_s = \frac{v}{c_s}$

Magnetization

$$\sigma \equiv \frac{B^2/4\pi}{(\gamma - 1)nmc^2} = \frac{1}{M_A^2} = \left(\frac{\omega_c}{\omega_p}\right)^2 \left(\frac{c}{v}\right)^2 = \left[\frac{c/\omega_p}{R_L}\right]^2$$

We explored the parameter space for pair and e-ion plasmas in 2D and 3D.

Low magnetization: shock mediated by Weibel instability, which generates field > background

High magnetization: shock mediated by magnetic reflection, compressing background

True for both pairs and e-ions, relativistic and nonrelativistic shocks

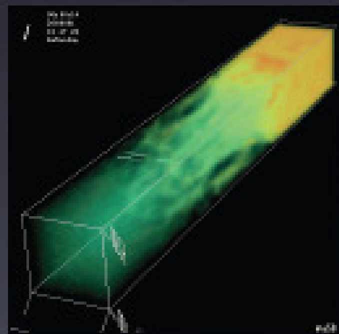

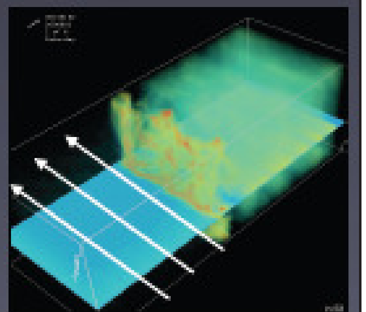

Can magnetized pair shocks accelerate particles?

Investigate the dependence of acceleration on the angle between the background field and the shock normal (Sironi & AS 08): σ=0.1, γ=15; Find p-law index near -2.3

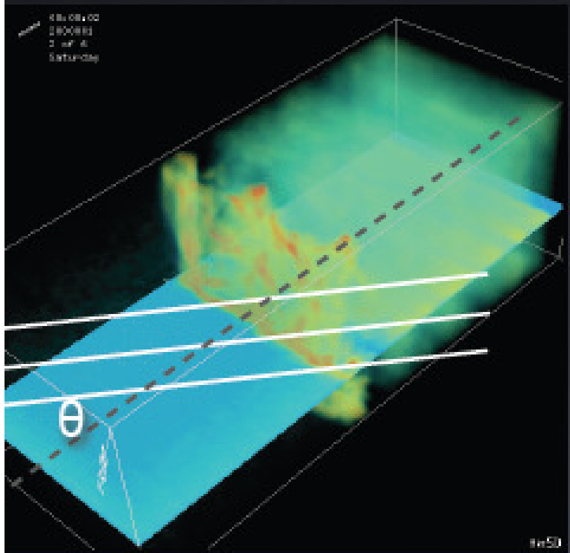

$\beta_{sh}/\cos\theta < 1$ -- subluminal

Self-turbulence is not enough to exceed superluminal constraint

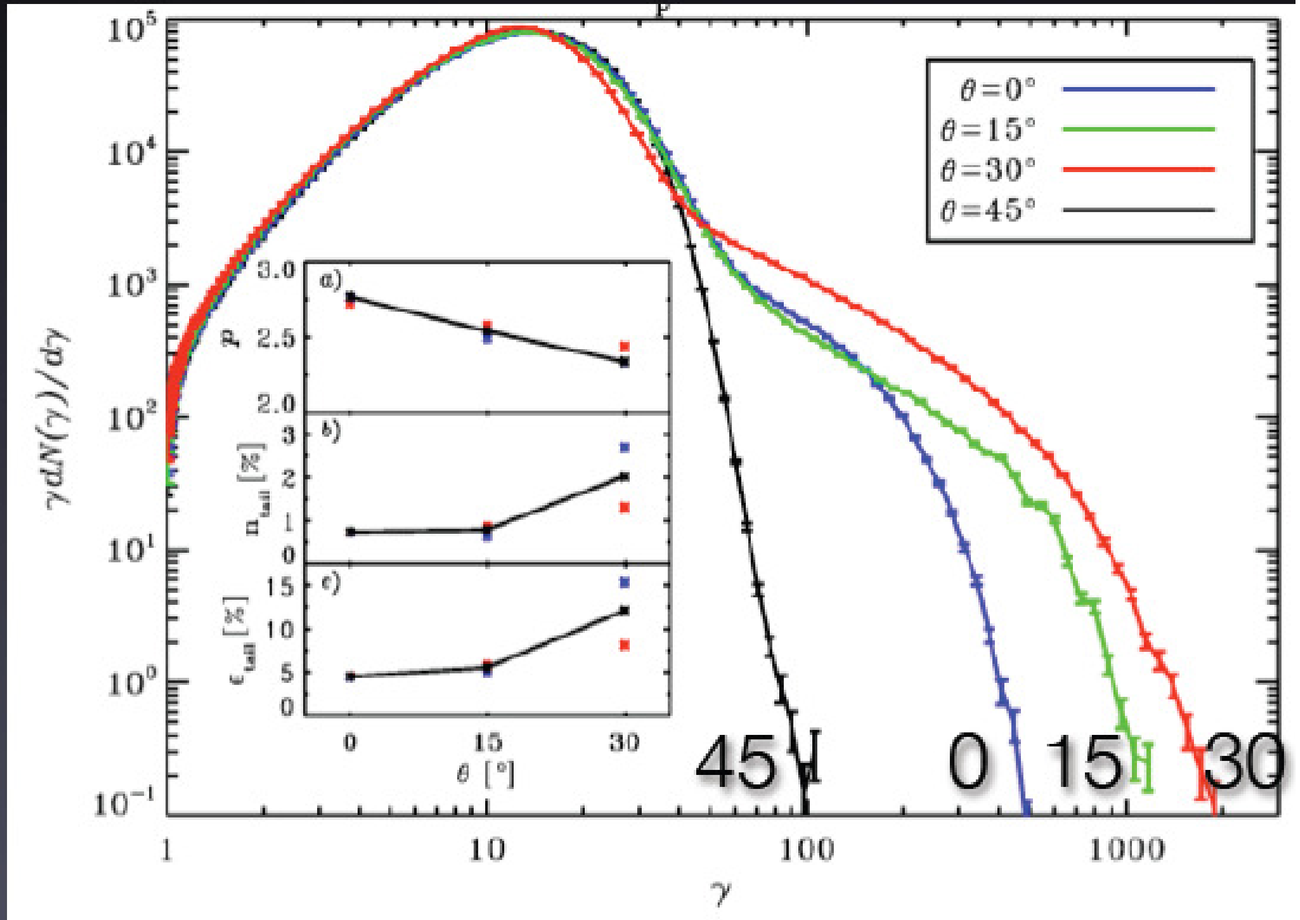

Observe transition between subluminal and superluminal shocks.
Shock drift acceleration is important near transition.

In upstream frame need:
$\theta_{upstream} < 32^\circ/\gamma$

Perpendicular shocks are poor accelerators

- **Particle acceleration:**

- **Injection problem and its association with the magnetic field structures**
- **Problem of efficiency of mechanisms: in astrophysics the gradient drift comes into the game for oblique shocks**
- **Multi-scales**
- **Diffusion scale**

Quasi-parallel Shock Studies

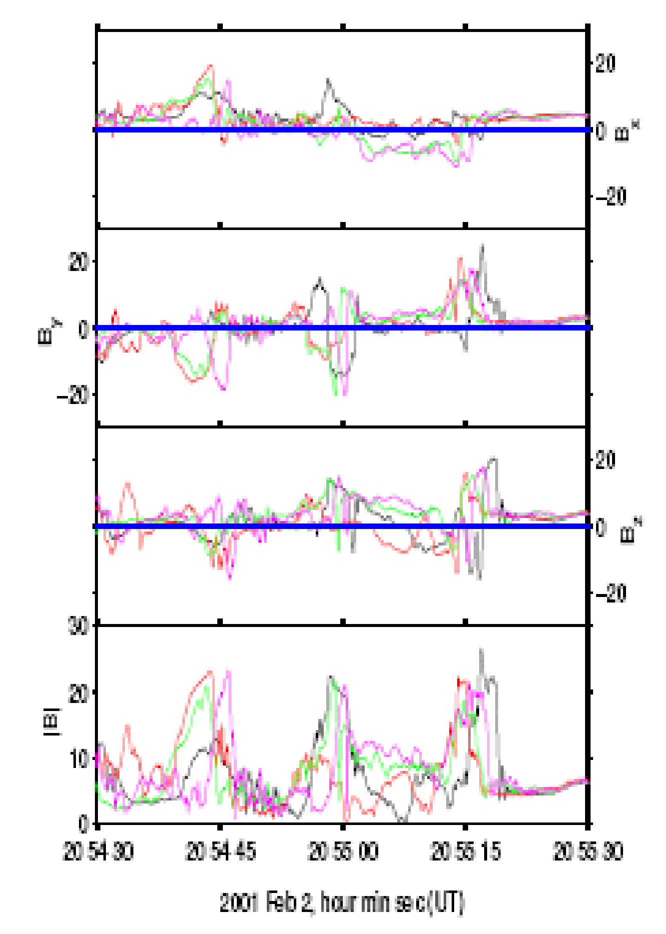

Lucek et al. 2002

- Quasi-parallel conditions allow particles to traverse shock, resulting in extended, turbulent transition
- Many pulsations or "Short Large Amplitude Magnetic Structures"
- SLAMS are ∼20 seconds, comparable to ULF foreshock wave periods, and driven by gradients in diffuse energetic ions
- ⇔ $1R_e$ or so in scale
- BUT Cluster scales of 600-800km show considerable variation
- Components, magnitudes, ...

SLAMS Coherence Scales

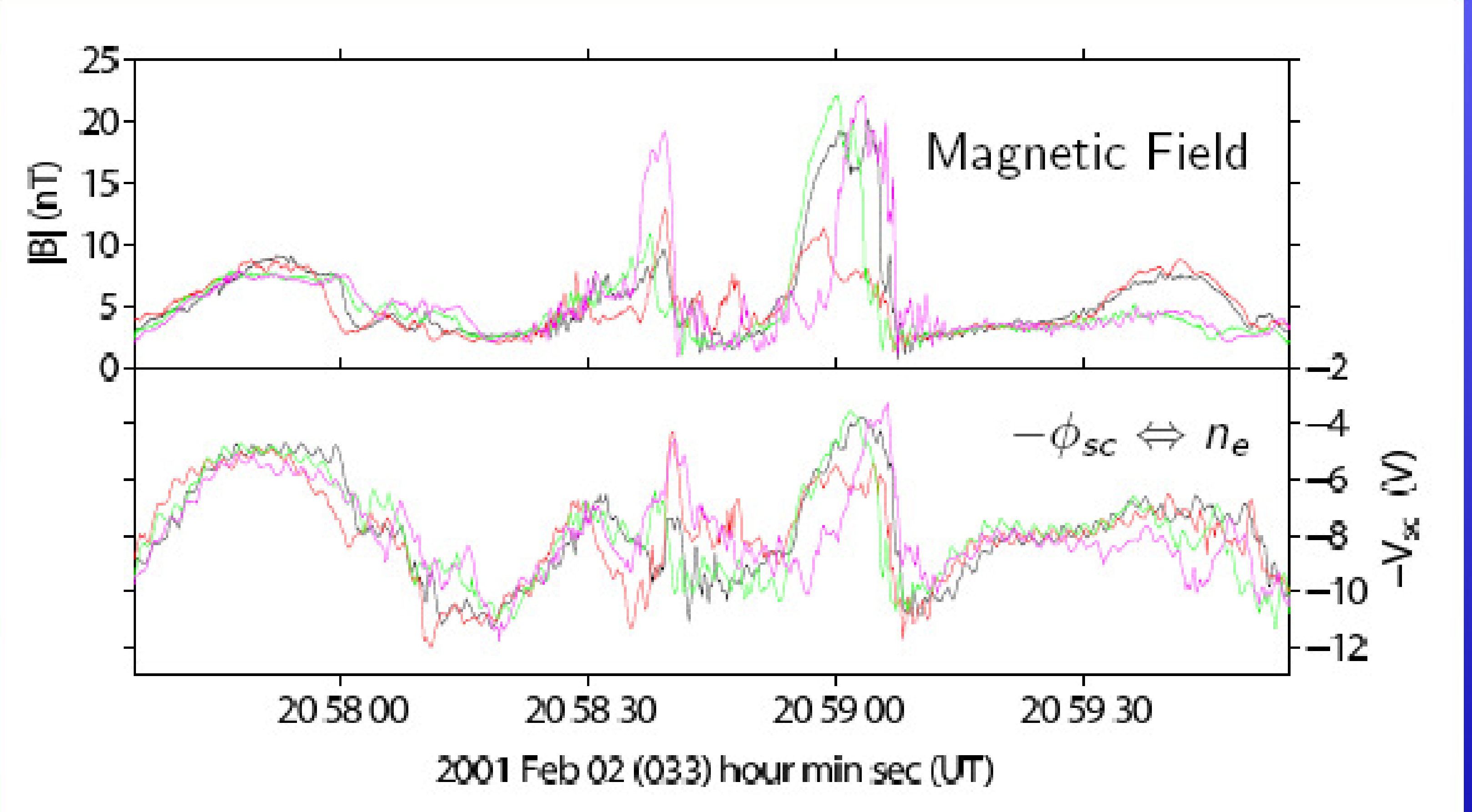

Lucek et al. 2004

Cluster tetrahedron ~ 600km

SLAMS Coherence Scales

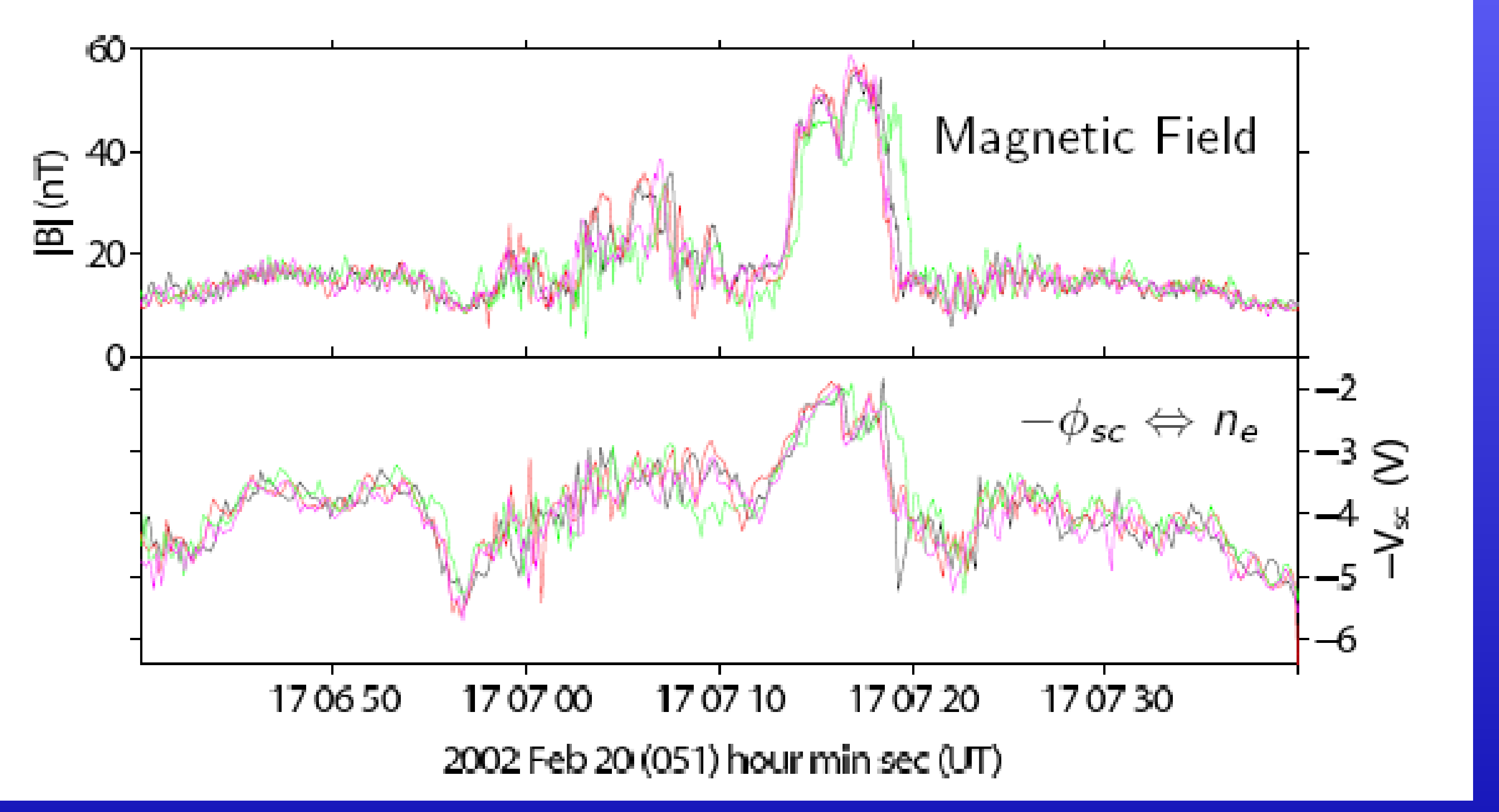

Lucek et al. 2004

Cluster tetrahedron ∼ 100km

Giacalone, Schwartz and Burgess, 1993

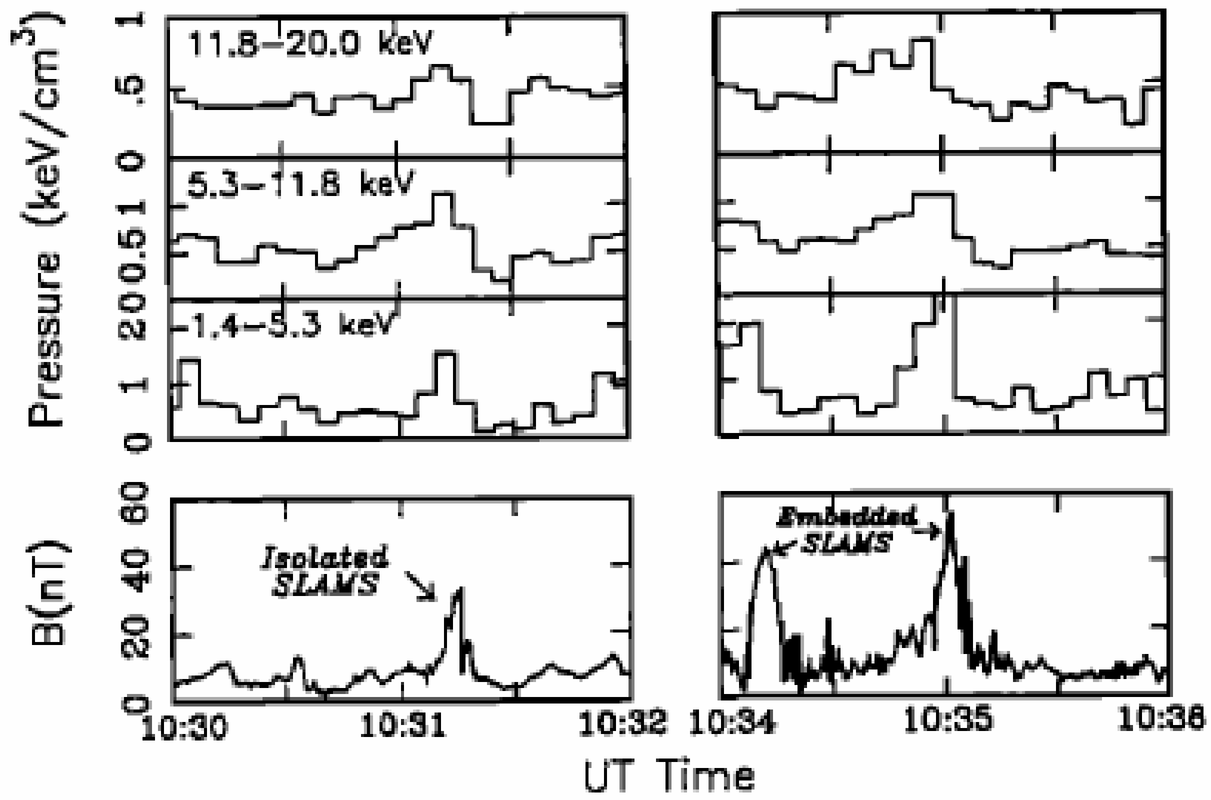

Fig. 1. Magnetic field magnitude and associated ion pressure signatures as viewed in the AMPTE/UKS spacecraft frame of reference of two SLAMS identified by Schwartz et al. [1992, c. f. Figures 6, 7, 14 and 15 which study the field structure and plasma signatures for these two events].

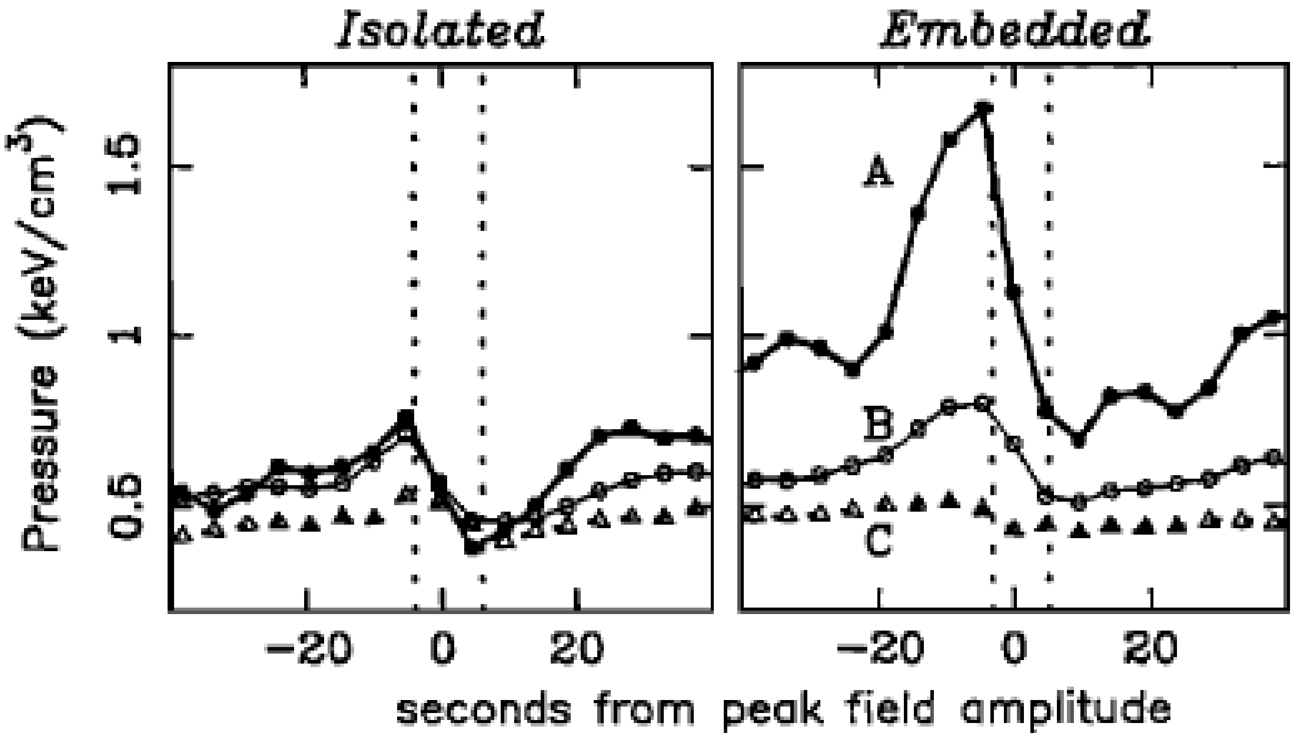

Fig. 4. Results of the superimposed epoch analysis of the spacecraft frame pressure for sub-populations of (A) 1.4–5.3 keV, (B) 5.3–11.8 and (C) 11.8–20 keV ions.

Ion events associated with different magnetic field features (Wilkinson et al, 1993)

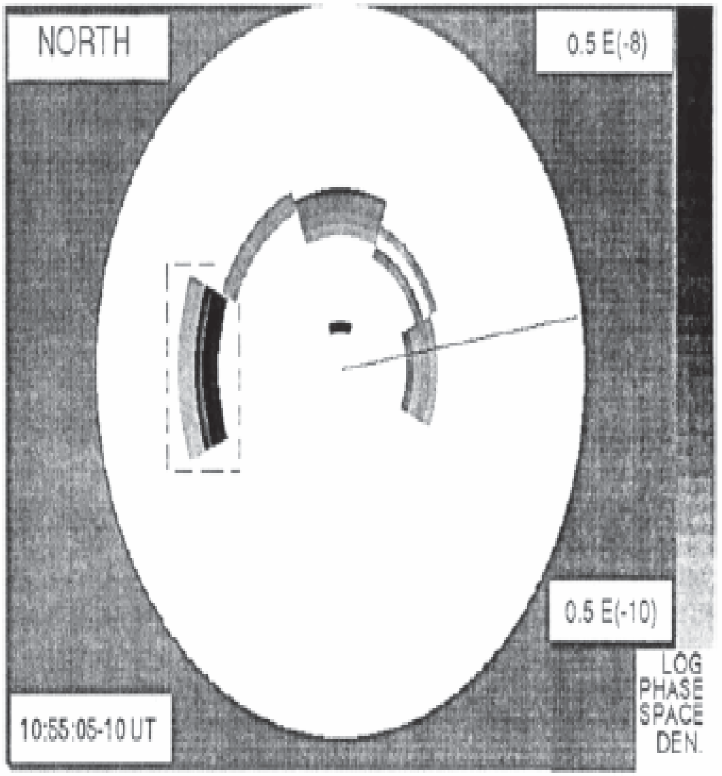

Fig. 4*a*. Dense ions observed over a wide range of azimuthal angles centered on the dusk direction, by detector displaying angles of propagation in excess of 22.5°N of the ecliptic. Format as in Figure 2*a*. The time of the measurements corresponds to the satellite rotation beginning at 1055:04.647.

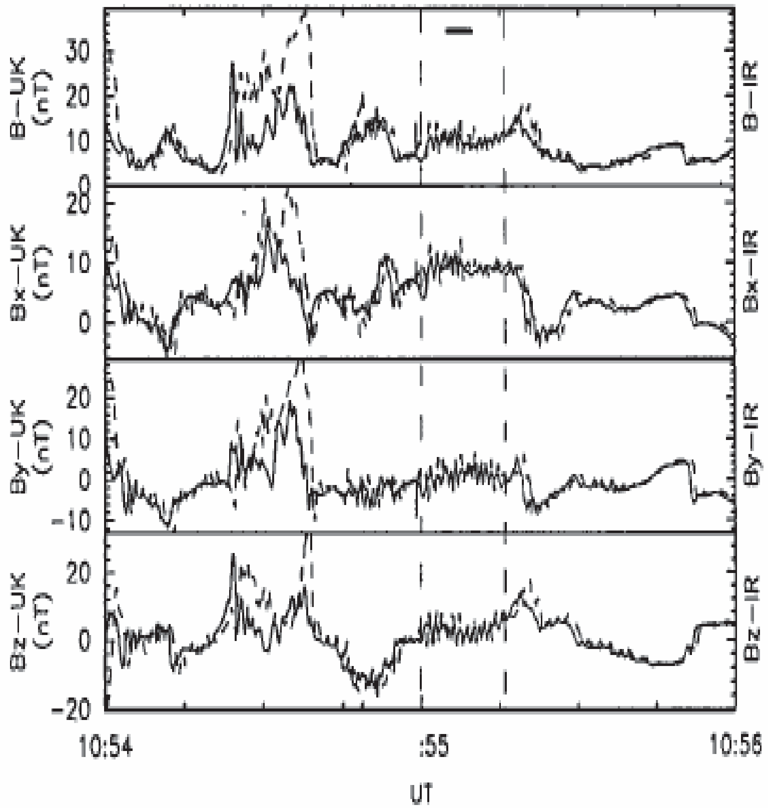

Fig. 4*b*. Magnetic field measurements as a function of time, during a 2-min interval encompassing the ion observations reported in Figure 4*a*. Format as in Figure 1*b*.

Real fields amplitudes

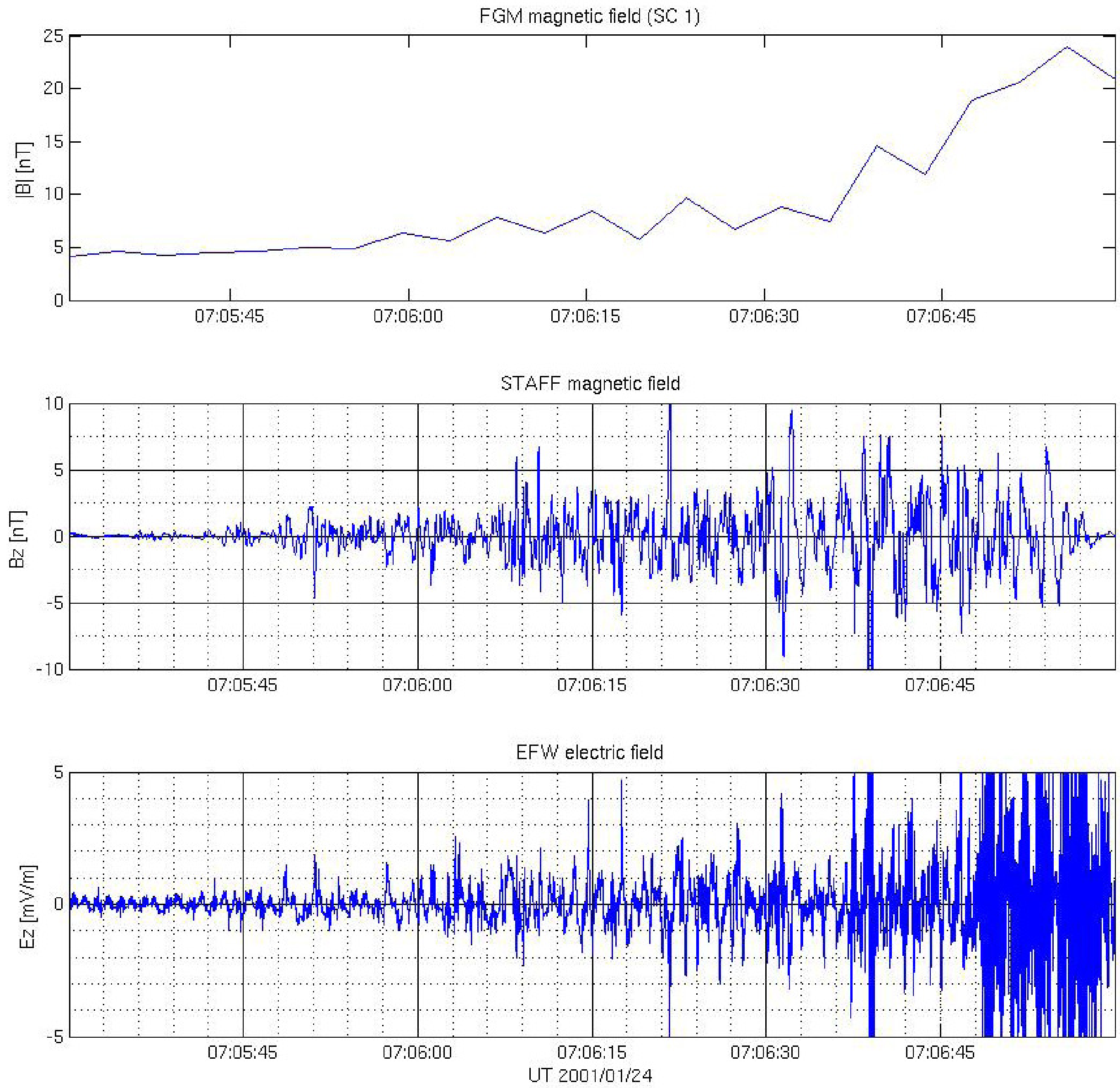

Simulation field amplitudes

$B = B / B_0$

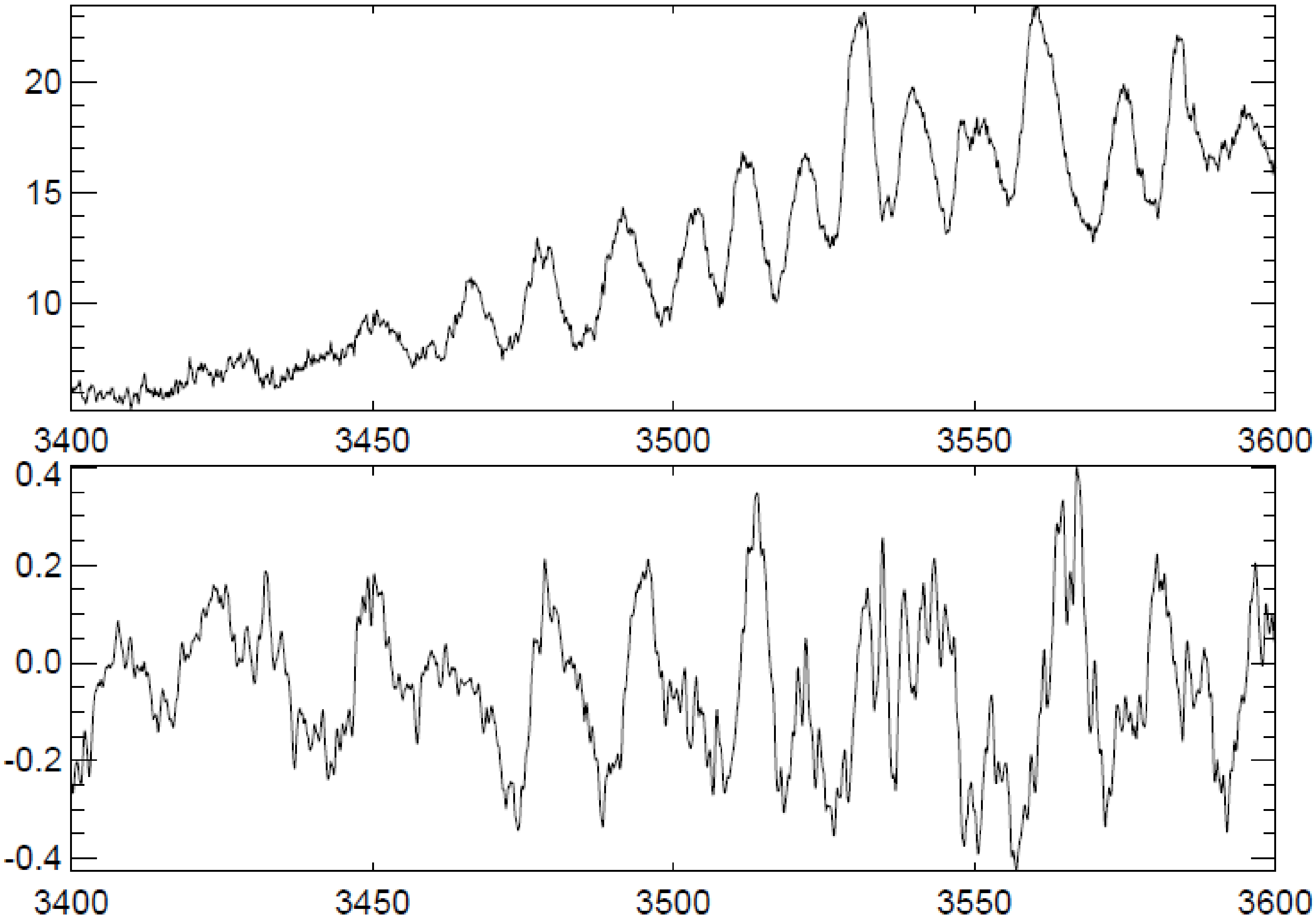

$e = E / 1.2 V/m$

Where is the difference between simulations and experiment

$$N = \frac{kc}{\omega}$$

$$rot\,\overrightarrow{E} = -\frac{\partial \overrightarrow{B}}{\partial t}$$

$$[\overrightarrow{k} \times \overrightarrow{E}] = \omega \overrightarrow{B}.$$

$$\frac{cB}{E} = \frac{kc}{\omega} = N.$$

$$N = \frac{c}{V_{ph}}. = \frac{c}{V_{SW}} = \frac{c}{MV_A}$$

$$N_{\exp} = \frac{Bc}{E} = \frac{c}{V_{SW}}\left(\frac{\omega_p}{\Omega_c} = \frac{2.7 * 10^4}{1.2 * 10^2} \sim 230\right) = 700$$

$$N_{sim} = N_{\exp}\left[\left(\frac{\omega_p}{\Omega_c}\right)_{sim} / \left(\frac{\omega_p}{\Omega_c}\right)_{\exp}\right] == 23$$

$$\delta E_{sim} / \delta E_{\exp} \sim 30$$

Parameters in PIC Simulations of Collsionless Shocks

1. Mass ratio m_i / m_e

2. Ratio of electron plasma to gyrofrequency $\nu = \frac{\omega_{pe}}{\Omega_{ce}} = \frac{c}{V_A}\sqrt{\frac{m_e}{m_i}}$

	m_i / m_e	$\omega_{pe} / \omega_{ce}$		c / V_A
Solar Wind	1836	100 – 200		(5000)
Biskamp and Welter, 1973	124	5	1-D	
Lembege and Dawson, 1987	100	2	1-D	
Liewer et al., 1991	1836	1-4	1-D	
Savoini and Lembege, 1994	42	2	2-D	
Shimada and Hoshino, 2000,2003,2005	20	20	1-D	(90)
Lembege and Savoini, 2002	42	2	2-D	
Krasnoselskikh et al., 2002	200	-	1-D	
Hada, Oonishi. Lembege, Savoini 2003	84	2	1-D	(18)
Scholer, Shinohara, Matsukiyo, 2003	1840	2	1-D	(95)
Scholer, Matsukiyo, 2004	1840	2	1-D	
Muschietti and Lembege, 2005	100	2	1-D	(20)
Matsukiyo, Scholer, 2006	1860	2	2-D	
Scholer, Comisel, Matsukiyo, 2007	1000	5	1-D	(150)